Size dependence of the ferroelectric transition of small $BaTiO_3$ particles: Effect of depolarization

Wan Y. Shih
Department of Chemical Engineering and Princeton Materials Institute, Princeton University, Princeton, New Jersey 08544 and Department of Materials Engineering, Drexel University, Philadelphia, Pennsylvania 19104

Wei-Heng Shih
Department of Materials Engineering, Drexel University, Philadelphia, Pennsylvania 19104

Ilhan A. Aksay
Department of Chemical Engineering and Princeton Materials Institute, Princeton University, Princeton, New Jersey 08544
(Received 18 May 1994; revised manuscript received 5 August 1994)

A theory has been developed to examine the depolarization effect on the ferroelectric transition of small $BaTiO_3$ particles. To reduce the depolarization energy, a crystal would break up into domains of different polarization. In this study, we consider cubic particles with alternating domains separated by 180° domain walls. The depolarization energy and the domain-wall energy were incorporated into the Landau-Ginzburg free-energy density. Assuming a hyperbolic tangent polarization profile across the domain wall, the domain-wall energy γ and the domain-wall half thickness ξ can be obtained by minimizing γ with respect to ξ. To account for $BaTiO_3$ not being a perfect insulator, a Schottky space charge layer beneath the particle surface that shields the interior of the crystal from the depolarization field was considered. The equilibrium polarization P and domain width D can be obtained by minimizing the total free-energy density with respect to both P and D. The results of the calculations show that the ferroelectric transition temperature of small particles can be substantially lower than that of the bulk transition temperature as a result of the depolarization effect. Consequently, at a temperature below the bulk transition temperature, the dielectric constant ϵ can peak at a certain cube size L. These results agree with the existing experimental observations. Finally, the theory can also be applied to other ferroelectric materials such as KH_2PO_4 or $PbTiO_3$.

I. INTRODUCTION

The effect of particle size on the ferroelectric phase transition and the dielectric properties of small $BaTiO_3$ particles has long been an interest of research. Experiments with submicrometer size $BaTiO_3$ and $PbTiO_3$ particles have revealed that particle size plays an important role on the paraelectric-to-ferroelectric transition and on the dielectric properties of small particles.[1–7] For example, early x-ray-diffraction (XRD) experiments on $BaTiO_3$ powders at room temperature showed a reduced c/a ratio of the tetragonal ferroelectric phase as the particle size was decreased below 1 μm.[1,2] More recent experiments on powder samples clearly showed that the paraelectric-to-ferroelectric transition temperature T_c decreases with a decreasing particle size. Ishikawa, Yoshikawa, and Okada[3] showed that the transition temperature T_c of $PbTiO_3$ particles decreases with a decreasing particle size as the particle size reaches about 500 Å by probing the softening of the transverse optical mode with Raman spectroscopy. Later, Uchino, Sadanaga, and Hirose[4] used x-ray diffractometry to show that the transition temperature T_c of $BaTiO_3$ particles also decreases with a decreasing particle size when the particle size is below 0.2 μm. Other researchers[5–7] have also reported similar observations that small $BaTiO_3$ particles are cubic at room temperature. However, the critical size below which $BaTiO_3$ particles become cubic seems to vary with the preparation methods.[6,7]

Meanwhile, the size dependence of the dielectric constant has also been observed in both $PbTiO_3$ composites[8] and in $BaTiO_3$ ceramics[9,10] and composites.[11] The dielectric constant of a composite of small $PbTiO_3$ particles in a conductive matrix (polymer with carbon) was shown to decrease with a decreasing particle size.[8] The authors suggested that the decrease in the dielectric constant with smaller $PbTiO_3$ particles is due to the lack of domain formation in the small particles.[8] The size dependence of the dielectric constant of $BaTiO_3$ ceramics is an intriguing one. It was shown that the dielectric constant exhibited a peak with respect to the grain size and the peak value of the dielectric constant was higher than the dielectric constant of a $BaTiO_3$ single crystal in either the c or a direction.[9,10] Moreover, with transmission electron microscopy (TEM), Arlt, Hennings, and de With[9] showed that the 90° domain width of the $BaTiO_3$ ceramics decreases with a decreasing grain size. When a $BaTiO_3$ crystal transforms from the cubic nonpolar phase to the tetragonal ferroelectric phase, it undergoes expansion in the c direction and contraction in the a direction. Overall, the crystal undergoes a volume expansion as it transforms to the ferroelectric phase. Therefore, a grain within a $BaTiO_3$ ceramic would experience a pressure exerted by the surrounding grains as the ceramic transforms from the nonpolar phase to the polar phase. Arlt, Hennings, and de With[9] suggested that the decrease in

the 90° domain width with a decreasing grain size is a result of minimizing the stress energy associated with the cubic-to-tetragonal phase transformation. They further attributed the increased dielectric constant with a decreasing grain size as a result of the increased volume fraction of the domain walls as the grain size becomes smaller. However, the theory of Arlt, Hennings, and de With[9] cannot explain why the dielectric constant of a ceramic sample decreased again as the grain size was further decreased; nor can they explain the decrease of T_c in the powder samples.

It is conceivable that stresses can develop in a ceramic sample since grains cannot expand freely as the ceramic transforms from the nonpolar phase to the polar phase and stresses may affect the dielectric behavior. However, unlike ceramic samples, powder samples in the polar phase should be stress free since particles can undergo a free expansion at the transition. It is unclear what causes the change in the transition temperature of powders as the particle size decreases. One possible explanation for the decrease in the transition temperature is the pressure effect. It is well known that the ferroelectric transition temperature of $BaTiO_3$ decreases with an increasing pressure.[12] Uchino, Sadanaga, and Hirose[4] suggested that the decrease of the transition temperature of small $BaTiO_3$ particles is a result of the higher pressure due to the decreased radius of curvature of the small particles. However, to produce the observed change in T_c, it would require the polar crystals to have a surface tension two orders of magnitude higher than that of a typical ceramic crystal.

A plausible explanation for $BaTiO_3$ and $PbTiO_3$ particles to have the observed decrease in T_c with a decreasing particle size is the depolarization effect. Batra, Wurfel, and Silverman[13] have shown that the ferroelectric transition of thin films can be strongly affected by the depolarization field. Depolarization has also been demonstrated to affect the transition temperature of small KH_2PO_4 (KDP) particles.[14] Experiments on KDP particles embedded in an insulating medium showed that particles smaller than 150 nm exhibited no ferroelectric transition at 123 K, in contrast to particles larger than 400 nm. By replacing the insulating medium with a conductive one, the transition of small KDP particles at 123 K was restored, demonstrating that the absence of the transition of small KDP particles in an insulating medium was due to the depolarization effect. Even though $BaTiO_3$ and $PbTiO_3$ are not perfect insulators, it is possible that the reduction of T_c in the small $BaTiO_3$ and $PbTiO_3$ particles is also due to the depolarization effect.

The reason that the depolarization effect suppresses the ferroelectric transition of small KDP particles is that it increases the energy of the polar phase. The depolarization energy can be reduced by domain formation or conduction. While the experiment on KDP particles qualitatively demonstrated the depolarization effect on the ferroelectric transition temperature of small particles, detailed knowledge about how the depolarization effect influences the ferroelectric transition of small particles is lacking. For example, how is the formation of domains within a particle affected by the size and conductivity of the particle? How does this in turn affect the transition temperature of the particle?

The purpose of this paper is to theoretically examine the depolarization effect on the paraelectric-to-ferroelectric transition of small particles. The approach is to include the terms associated with depolarization in the Ginzburg-Landau free-energy density[2,14,15] of a particle. The calculations will be carried out for $BaTiO_3$, since the coefficients of the Ginzburg-Landau free energy for $BaTiO_3$ are well known.[2,14,15] To reduce the electrostatic energy due to the depolarization field, the crystal would break up into domains of different polarizations. Therefore, the energy associated with depolarization should include (1) the energy due to the depolarization field and (2) the energy of the domain walls. For simplicity, we only consider cubic particles with planar domains separated by 180° domain walls in this paper. It should be noted that for $BaTiO_3$ both 90° and 180° domain walls can occur in the tetragonal phase; the shape of the particles is not exactly cubic, and the domains may not be planar. Nonetheless, the present approach is an attempt to qualitatively give an estimate of the depolarization effect on the ferroelectric transition of small particles. Considerations of other particle geometries (e.g., spheres) or other types of domain walls would only modify the quantitative results slightly.

For a given cubic particle size at a given temperature, the equilibrium polarization and the equilibrium domain width can be obtained by minimizing the total free-energy density with respect to both the polarization and domain width. Since the theory involves the energy of the 180° domain walls, to be self-consistent, we also calculate the domain-wall energy within Ginzburg-Landau theory. For a given polarization, assuming a hyperbolic tangent polarization profile with the domain-wall thickness as a variable, the domain-wall energy can be obtained by minimizing the domain-wall energy with respect to the domain-wall thickness. To take into account the fact that particles are not perfect insulators, a Schottky-type space-charge layer near the surface[14–17] that shields the interior of the particles from the depolarization field is also considered. The results of the calculations are compared to the existing experiments. It should be noted that the depolarization effect has no counterpart in ferromagnetic crystals, as the magnetostatic self-energy is about 10^3 times smaller than the transition energy and thus cannot suppress the spontaneous magnetization.[14]

The rest of the paper is organized as follows. Section II contains the theory. The results of the calculations and a discussion are given in Sec. III. Concluding remarks are given in Sec. IV.

II. THEORY

For a crystal that undergoes a paraelectric-ferroelectric transition, the total free-energy density (free energy per unit volume) F may be separated into two parts:

$$F = F(P) + F_0 , \tag{1}$$

where P denotes the polarization, $F(P)$ the part of the free-energy density that arises from a nonzero polarization, and F_0 the part of the free-energy density that is not related to the polarization. According to the theory of Ginzburg and Landau,[2,14,15] $F(P)$ can be expanded in terms of P. Many ferroelectric materials such as perovskite ferroelectrics undergo a first-order transition as temperature is lowered below the transition temperature T_c. Therefore, it is necessary to expand the polar part of the free-energy density $F(P)$ at least to the sixth order in P as[2,14,15]

$$F(P)=\frac{\alpha}{2}P^2+\frac{\beta}{4}P^4+\frac{\sigma}{6}P^6 , \tag{2}$$

where the coefficient $\alpha=a(T-T_{0\infty})$, with a being the inverse of the Curie constant and $T_{0\infty}$ the Curie-Weiss temperature, and the coefficients β and σ for the fourth- and sixth-order terms are more or less constant. The equilibrium P is determined by minimizing Eq. (2) with respect to P. For $BaTiO_3$ crystals, the numerical values for the coefficients α, β, and σ are well known. However, Eq. (2) only describes the polar part of the bulk free-energy density of large single-domain crystals and it does not include the energy contribution associated with depolarization. It is the purpose of this paper to incorporate the depolarization contribution into Eq. (2).

A. Depolarization energy

For simplicity, let us consider a cubic crystal. If the crystal is a perfect insulator and has only one single domain with polarization P, the polarization would lead to surface charges on the top and bottom surfaces as illustrated in Fig. 1(a), resulting in a depolarization field $E_1=-4\pi P$ whose direction is opposite to that of P. Therefore, the depolarization energy per unit volume is

$$E_d=-\int_0^P E_1 dP'=2\pi P^2 , \tag{3}$$

and for a single-domain crystal, the total polar part of the free-energy density should then be

$$F_{\text{tot}}(P)=F(P)+2\pi P^2 . \tag{4}$$

The depolarization energy E_d is negligible when P is small. However, ferroelectrics generally have high polarization. The polarization of perovskite ferroelectric crystals is on the order of 10^5 esu/cm^2. To reduce the depolarization energy in the ferroelectric state, the crystals tend to break up into domains of different polarization. It was shown that when a cube of side L breaks up into domains of alternating slices of up polarization and down polarization with a domain width D as illustrated in Fig. 1(b), the depolarization energy per unit volume is reduced to[18]

$$E_d=1.7P^2\frac{D}{L} . \tag{5}$$

By breaking up into domains, the depolarization energy of a crystal is reduced by a factor of D/L in addition to a constant numerical factor. Meanwhile, the breakup creates domain walls. Let γ denote the domain-wall energy. Including the domain-wall contribution, the total depolarization-energy density of a multiple-domain cube is then

$$E_d=1.7P^2\frac{D}{L}+\gamma\left[\frac{L}{D}-1\right]\frac{1}{L} . \tag{6}$$

Equations (5) and (6) are valid if the domain-wall thickness is negligible compared to the domain width D.[18]

B. Space-charge layer

Note that Eqs. (3)–(6) are good for perfect insulators. If the crystal is not a perfect insulator, a space-charge layer at the surface can affect the ferroelectric properties of the crystal. The existence of a space-charge layer near the surface of $BaTiO_3$ has been studied by many investigators using various techniques. These experiments can be found in many reviews.[14–17] Space-charge layers can be due to surface ionic vacancies as suggested by Känzig[2,19] or to Schottky exhaustion barriers[20] as suggested by Triebwasser.[21] In this paper, we will consider the Schottky space-charge layer that effectively shields the interior of the crystal from the depolarization field. The width of the Schottky barrier depends on the charge-carrier concentration. Generally, it was estimated that for $BaTiO_3$ the thickness of the space-charge layer ranges from 10^2 to 10^4 Å, depending on the mobile charge-carrier concentration.[14–17] In general, the charge distribution within the layer is nonuniform.[13,22] In the present paper, for simplicity, we will assume a Schottky type of space-charge layer. The charge density within the layer is uniform as illustrated in Fig. 2. Let t denote the thickness of the space-charge layer, and let us first consider a single-domain crystal for the convenience of dis-

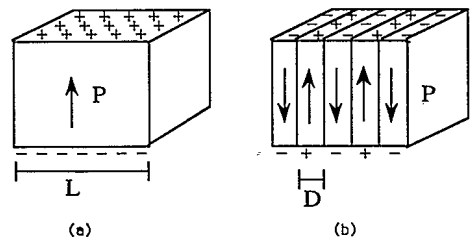

FIG. 1. (a) A cubic crystal of size L with one single domain of polarization P. (b) A crystal of size L with domains of alternating polarization separated by 180° domain walls. The domain width is D.

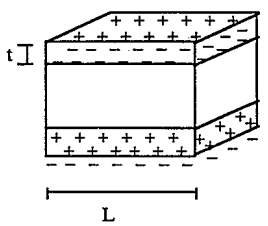

FIG. 2. Space-charge layers of thickness t with uniform charge distribution.

cussion. Assuming that the surface-charge density due to the polarization is totally balanced by the opposite charges within the layer, the charge density ρ in the space-charge layer would then be

$$\rho=\frac{-P}{t} . \tag{7}$$

The electric field E in the layer is then

$$E=\frac{-4\pi P}{t}(t-z) \quad \text{for } 0<z<t , \tag{8}$$

and $E=0$ outside of the layer. Therefore, for a single-domain crystal, the depolarization-energy density is modified as

$$E_d=-2\int_0^P\int_0^t\frac{-4\pi P'}{t}(t-z)dz\,dP'/L=2\pi P^2\frac{t}{L} , \tag{9}$$

where the factor 2 takes into account that there are two space-charge layers, one at the top and the other at the bottom. The consideration of a Schottky space-charge layer of thickness t modifies the depolarization-energy density by a factor t/L. Applying the same analysis for multiple-domain crystals, the total depolarization energy depicted in Eq. (6) becomes

$$E_d=1.7P^2\frac{D}{L}\frac{t}{L}+\gamma\left[\frac{L}{D}-1\right]\frac{1}{L} . \tag{10}$$

C. 180° domain walls

There have been quite a number of theoretical calculations for both 90° and 180° domain-wall energies of $BaTiO_3$.[23–28] In the present paper, we are only concerned with the 180° domain walls. To be consistent with the Ginzburg-Landau theory we used for this study, we will calculate the energies of the 180° domain walls within Ginzburg-Landau theory. If the polarization is nonuniform, the polar part of the free-energy density at position $\mathbf{r}$ becomes a functional of $\mathbf{P}(\mathbf{r})$ as

$$\mathbf{F}(\mathbf{P}(\mathbf{r}))=\frac{\alpha}{2}\mathbf{P}(\mathbf{r})^2+\frac{\beta}{4}\mathbf{P}(\mathbf{r})^4+\frac{\sigma}{6}\mathbf{P}(\mathbf{r})^6+c|\nabla\mathbf{P}(\mathbf{r})|^2 . \tag{11}$$

If a domain wall is located at $x=0$, assuming that $\mathbf{P}$ is a function of x only and is independent of y and z, one can define the domain-wall energy γ as

$$\gamma=\int_{-\infty}^{\infty}\Delta\mathbf{F}(\mathbf{P}(x))dx , \tag{12}$$

where $\Delta F(\mathbf{P}(x))=\mathbf{F}(\mathbf{P}(x))-F(P)$, where P and $F(P)$ denote the bulk polarization and the bulk free-energy density, respectively. The equilibrium polarization profile $\mathbf{P}(x)$ across the wall can be obtained by requiring

$$\int_{-\infty}^{\infty}\frac{\partial\Delta\mathbf{F}(\mathbf{P}(x))}{\partial\mathbf{P}(x)}dx=0 . \tag{13}$$

We will assume that the polarization profile $\mathbf{P}(x)$ is a hyperbolic tangent function of x, i.e.,

$$\mathbf{P}(x)=P\tanh(x/\xi) , \tag{14}$$

where P denotes the bulk polarization and ξ the half width of the wall. A schematic of a 180° domain wall is shown in Fig. 3. With Eq. (14), the domain-wall energy minimization requirement shown in Eq. (13) becomes

$$\frac{\partial\gamma}{\partial\xi}=0 . \tag{15}$$

Therefore, given a bulk polarization P, the equilibrium domain-wall polarization profile $\mathbf{P}(x)$ and the domain-wall energy can be obtained by minimizing γ with respect to ξ. Note that the hyperbolic tangent domain-wall polarization profile of Eq. (14) is a reasonable approximation considering that (i) the equilibrium domain-wall polarization profile is hyperbolic tangent if the free-energy density is a fourth-order function of the polarization, i.e.,

$$F(\mathbf{P}(x))=\frac{\alpha}{2}\mathbf{P}(x)^2+\frac{\beta}{4}\mathbf{P}(x)^4+c|\nabla\mathbf{P}(x)|^2 ,$$

and (ii) experimental domain-wall profiles obtained by electron holograms[29] agreed fairly well with a hyperbolic tangent one. With $\mathbf{P}(x)=P\tanh(x/\xi)$, the domain-wall energy γ between two semi-infinite domains can be written as

$$\gamma=-\alpha\xi P^2-\frac{2}{3}\xi\beta P^4-\frac{23}{45}\xi\sigma P^6+\frac{4}{3}\frac{c}{\xi}P^2 . \tag{16}$$

The half thickness of a wall between two semi-infinite domains can be obtained analytically by minimizing γ with respect to ξ:

$$\xi=[\tfrac{4}{3}c(-\alpha-\tfrac{2}{3}\beta P^2-\tfrac{23}{45}\sigma P^4)^{-1}]^{1/2} . \tag{17}$$

Once the domain-wall half thickness is known, the domain-wall energy may simply be rewritten as

$$\gamma=\frac{8}{3}\frac{c}{\xi}P^2 . \tag{18}$$

For multiple-domain crystals with a domain width D and the polarization at the center of a domain P, the domain-wall energy becomes

$$\gamma=\int_{-D/2}^{D/2}[\mathbf{F}(\mathbf{P}(x))-F(P)]dx \tag{19}$$

and can be written analytically as

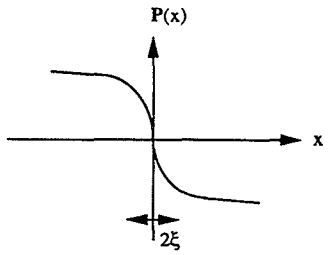

FIG. 3. Schematic of a hyperbolic tangent polarization profile across a 180° domain wall. The domain-wall thickness is 2ξ, where ξ is as defined in the text.

$$\gamma=-a_1\xi(\alpha P^2)-a_2\xi\left[\frac{1}{2}\beta P^4\right]-a_3\xi\left[\frac{1}{3}\sigma P^6\right]+a_4\left[2\frac{c}{\xi}P^2\right], \tag{20}$$

where

$$\begin{aligned} a_1&=\tanh^{-1}(D/2\xi)\,,\\ a_2&=\tanh^{-3}(D/2\xi)[1+\tfrac{1}{3}\tanh^2(D/2\xi)]\,,\\ a_3&=\tanh^{-5}(D/2\xi)[1+\tfrac{1}{3}\tanh^2(D/2\xi)+\tfrac{1}{5}\tanh^4(D/2\xi)]\,,\\ a_4&=\tanh^{-1}(D/2\xi)[1-\tfrac{1}{3}\tanh^2(D/2\xi)]\,. \end{aligned} \tag{21}$$

In the limit $D\gg 2\xi$,

$$\begin{aligned} a_1&=1+2e^{-D/4\xi}\,,\\ a_2&=\tfrac{4}{3}+\tfrac{20}{3}e^{-D/4\xi}\,,\\ a_3&=\tfrac{23}{15}+\tfrac{186}{15}e^{-D/4\xi}\,,\\ a_4&=\tfrac{2}{3}+\tfrac{4}{3}e^{-D/4\xi}\,. \end{aligned} \tag{22}$$

Therefore, for a finite domain width D, the domain-wall energy not only depends on the domain-wall half thickness ξ, but also the domain width D. However, as we will show below, it turns out that ξ is much smaller than D. Therefore, the modification of γ and ξ due to a finite D is rather limited as can be seen from Eqs. (20)–(22).

D. Free-energy density of a multiple-domain crystal

Combining Eqs. (2) and (10), the polar part of the free-energy density of a multiple-domain crystal of size L can be written as

$$F(P,D,L)=\frac{\alpha}{2}P^2+\frac{\beta}{4}P^4+\frac{\sigma}{6}P^6+1.7P^2\frac{D}{L}\frac{t}{L}+\gamma\left[\frac{L}{D}-1\right]\frac{1}{L}\,, \tag{23}$$

with γ being depicted in Eqs. (20)–(22). Thus, for a given crystal size L, the equilibrium polarization P and the domain width D can be determined by minimizing the free-energy density $F(P,D,L)$ with respect to P and D, i.e.,

$$\frac{\partial F(P,D,L)}{\partial P}=0 \tag{24}$$

and

$$\frac{\partial F(P,D,L)}{\partial D}=0\,. \tag{25}$$

Once the equilibrium polarization P is obtained, the dielectric constant can be obtained by

$$\epsilon=4\pi\chi+1\,, \tag{26}$$

where χ is the dielectric susceptibility defined as

$$\chi^{-1}=\frac{\partial^2 F(P,D,L)}{\partial P^2}\,. \tag{27}$$

The minimization of F with respect to D, i.e., Eq. (25), gives

$$D=\left[\frac{\gamma}{1.7P^2}\right]^{1/2}L^{1/2}\left[\frac{L}{t}\right]^{1/2}\,. \tag{28}$$

From Eq. (28), one can see that for a given polarization the domain width D is roughly proportional to the particle size L. Note that if there is no consideration for the space-charge layer, D would be proportional to $L^{1/2}$. The consideration of a Schottky-type space-charge layer that totally balances the surface charge changes the dependence of D from $L^{1/2}$ to L. If we consider a more realistic charge distribution, D may not be exactly linear in L. However, it is fair to say that if we assume $D\sim L^{\nu}$, the exponent ν must be larger than $\frac{1}{2}$. In the TEM experiment of Arlt, Hennings, and de With,[9] the domain width as a function of the grain size in a double-logarithmic plot indeed appeared to have a slope larger than $\frac{1}{2}$.

Finally, the effect of the depolarization energy and the domain-wall energy on the transition temperature of small cubic crystals of size L can be qualitatively understood as follows. With the depolarization energy $1.7P^2(D/L)(t/L)$ and the domain-wall energy $\gamma(L/D-1)/L$, the coefficient of the P^2 term in the free-energy density is no longer $\alpha=a(T-T_{0\infty})$ but α'. For simplicity, let us assume $\xi\ll D$, so that $\tanh(D/2\xi)\approx 1$, which is indeed the case as we will show in the following section. Using Eq. (16) for γ, one finds

$$\alpha'=\alpha+3.4\frac{Dt}{L^2}+\left[-\frac{2\xi}{D}\alpha+\frac{8}{3}\frac{c}{\xi}\right]. \tag{29}$$

Rewriting $\alpha'=a'(T-T_0)$, one obtains

$$a'=a\left[1-\frac{2\xi}{D}\right] \tag{30}$$

and

$$T_0=T_{0\infty}-\frac{1}{a'}\left[1.7\frac{Dt}{L^2}+\frac{8}{3}\frac{c}{\xi}\right]. \tag{31}$$

Equation (31) shows that as the crystal size L is reduced, the Curie-Weiss temperature and hence the transition temperature T_c are lowered.

III. RESULTS AND DISCUSSION

The coefficients α, β, and σ in the Landau-Ginzburg free energy can be obtained from the literature. The coefficient α for the P^2 term is related to the Curie constant and the Curie-Weiss temperature as $\alpha=a(T-T_{0\infty})$, where $T_{0\infty}$ is the bulk Curie-Weiss temperature and a the inverse of the bulk Curie constant. For $BaTiO_3$, above and near the bulk transition temperature $T_{c\infty}$, the coefficient β of the P^4 term has a mild tem-

TABLE I. Coefficients of the Landau-Ginzburg free energy of $BaTiO_3$.

$T_{c\infty}$	122 °C
$T_{0\infty}$	112 °C
a	7.4×10^{-5}
β	1.13×10^{-12}
σ	3.34×10^{-22}
c	0.3×10^{-16}

perature dependence and can be written as $\beta=18\times10^{-15}(T_{0\infty}-T_2)$ with $T_2=175$ °C. However, it is not clear what value β should be at lower temperatures. In this paper, we use $\beta=18\times10^{-15}\ (T_{0\infty}-T_2)$ for all temperatures. This β value gives very good quantitative agreement between the calculated polarization-temperature curve and the experimental one for bulk $BaTiO_3$. The quantitative values for a, $T_{c\infty}$, $T_{0\infty}$, β, and σ are listed in Table I.

A. 180° domain walls

To calculate the domain-wall polarization profile and the domain-wall energy, one needs to know the coefficient c for the gradient term in Eq. (11). However, the coefficient c is not known. Recent electron holographic experiments[29] on $BaTiO_3$ showed that at room temperature a 90° domain wall has a thickness of about 20 Å. If one assumes that the thickness of a 180° domain wall is roughly the same as that of a 90° one, then Eq. (17) can be used to estimate the coefficient, i.e.,

$$c=\tfrac{3}{4}\xi^2(-\alpha-\tfrac{2}{3}\beta P^2-\tfrac{23}{45}\sigma P^4)\ . \tag{32}$$

Using a polarization $P=78\,000$ esu/cm^2 and $2\xi=18$ Å at $T=25$ °C and the coefficients α, β, and σ listed in Table I, $c=0.3\times10^{-16}$. Plugging this c value back into Eq. (16), we obtain a domain-wall energy $\gamma=5.3$ ergs/cm^2 for $P=78\,000$ esu/cm^2 and $2\xi=18$ Å at $T=25$ °C, which is in line with the existing theoretical calculations,[23–26] which ranges 1–10 ergs/cm^2 for the 180° domain walls in $BaTiO_3$. Therefore, we feel that $c=0.3\times10^{-16}$ is a fairly good representation for the coefficient of the gradient term.

B. Multiple-domain crystals

For multiple-domain crystals, the results shown below were for the space-charge layer thickness $t=75$, 100, 167, and 500 Å. The layer thickness is related to the charge-carrier concentration. A smaller t represents a higher charge-carrier concentration (i.e., higher electrical conductivity). We will discuss more about the space-charge layer thickness in Sec. IV. To show the effect of particle size on the transition temperature T_c, Fig. 4 shows the polarization P as a function of temperature T for $L=0.4$, 0.5, 0.6, 0.7, 0.8, 2.0, and 1000 μm with $t=500$ Å. As L becomes smaller, the transition temperature T_c is decreased. Note that although the transition temperature is lowered, the first-order nature of the transition is unchanged. Furthermore, the polarization P at T_c is about 55 000 esu/cm^2 for all L. The reason for the more or less constant P at T_c for all L will be discussed in the next section. For ferroelectric crystals such as $BaTiO_3$, it is known that the spontaneous strain $(c/a-1)$ is proportional to the square of the spontaneous polarization.[14] The constant P at T_c for all L shown in Fig. 4 suggests that $(c/a-1)$ should also be constant at T_c regardless of the particle size. Indeed, the experiment of Uchino, Sadanaga, and Hirose[4] showed a constant $(c/a-1)$ at T_c for all the particle sizes studied.

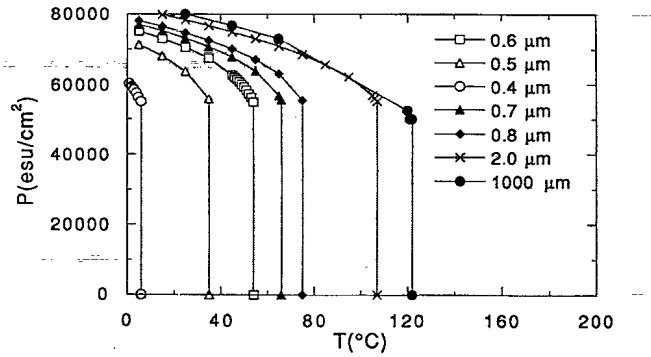

FIG. 4. P vs T for various L (in μm) with $t=500$ Å. Note that the drop of P at T_c is roughly the same for all L.

Meanwhile, from Fig. 4, one can see that at a given temperature, e.g., 25 °C, the polarization decreases with a decreasing L. Since the spontaneous strain $(c/a-1)$ is proportional to the square of the spontaneous polarization, the decreased P with a decreasing L shown in Fig. 4 should also indicate a decrease of $(c/a-1)$ with a decreasing particle size. In Fig. 5, we plot the room-temperature $(P/P_\infty)^2$ as a function of L for $t=75$, 100, 167, and 500 Å where P_∞ is the bulk polarization. P does not change significantly with L at large L until L is reduced to a certain size below which P decreases sharply. Moreover, below a critical size L_c, the crystal becomes nonferroelectric at room temperature. The critical

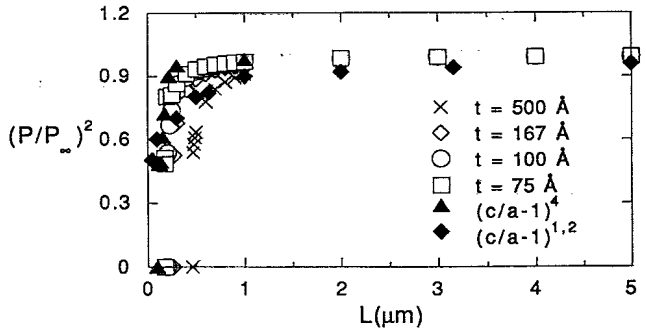

FIG. 5. $(P/P_\infty)^2$ vs L for $t=75$, 100, 167, and 500 Å. Also plotted are the experimental $(c/a-1)/(c/a-1)_\infty$ from Uchino, Sadanaga, and Hirose (Ref. 4) and Känzig and co-workers (Refs. 1 and 2), where $(c/a-1)_\infty$ denotes the bulk $(c/a-1)$ value.

size L_c depends on the value of t: $L_c=0.45$, 0.26, 0.2, and 0.175 μm for $t=500$, 167, 100, and 75 Å, respectively. As t becomes smaller, the ferroelectric phase can remain stable to a smaller particle size. This qualitatively explains why different authors seem to observe different size dependence. Also plotted in Fig. 5 are the experimental $(c/a-1)/(c/a-1)_\infty$ for comparison: solid triangles from Uchino, Sadanaga, and Hirose[4] and solid diamonds from Anliker, Brugger, and Känzig, where $(c/a-1)_\infty$ denotes the bulk $(c/a-1)$ value. One can see the different size dependence of $(c/a-1)$ among the two experiments.

In Fig. 6, we plot T_c as a function of L for $t=500$, 167, 100, and 75 Å. Again, T_c does not change much at large L, but decreases sharply below a certain L, similar to the behavior of P versus L shown in Fig. 5. Also plotted in Fig. 6 are the data points from the experiment of Uchino, Sadanaga, and Hirose.[4] Note that even though the $(c/a-1)/(c/a-1)_\infty$ curve of Uchino, Sadanaga, and Hirose appears to coincide with the calculated curve of $(P/P_\infty)^2$ for $t=75$ Å as shown in Fig. 5, the change in T_c in the experimental system of Uchino, Sadanaga, and Hirose is much more abrupt than the calculated curve of T_c versus L for $t=75$ Å when the particle size is around 0.1–0.2 μm. One possible explanation for the more abrupt change of T_c in the experiment is that the particle size in the experimental system has a distribution. Since larger particles have a higher T_c, the observed transition temperature T_c of particles that have a size distribution would be determined by that of the largest particles in the distribution rather than that of the average-size particles. Therefore, experimentally, T_c would be very sensitive to the particle-size distribution. On the other hand, the quantity $(c/a-1)$ at a certain temperature is an averaged quantity over all particles and is, therefore, not as sensitive to the presence of the larger particles. As a result, experimentally, one may not see the same size dependence between $(c/a-1)$ and T_c.

Meanwhile, the shape of the particles also has an effect on the size dependence. It is known that the depolarization factor of a single-domain spherical particle is one-third of that of a single-domain cubic particle. It is not known what the depolarization factor of a multiple-domain spherical particle would be. However, it can be expected that for multiple-domain crystals, spheres would also have a lower depolarization factor than cubes. Therefore, the ferroelectric phase can be stable to a smaller particle size with a sphere than with a cube. If one assumes that the depolarization of a multiple-domain sphere is also one-third of that of a multiple-domain cube, then the effect of $t=167$ Å for a cube would be equivalent to that of $t=500$ Å for a sphere of the same size. That is, at room temperature, a cube with $t=500$ Å would become nonpolar for $L\leq 0.45$ μm, whereas a sphere with $t=500$ Å would not become nonpolar until $L\leq 0.26$ μm (Fig. 5). Similar to an infinitely large system, the dielectric constant ϵ of a small crystal also reaches a very high value at T_c. As an example, we plot the polarization P and the dielectric constant ϵ as a function of T for $L=0.6$ μm and $t=500$ Å in Fig. 7. As we have discussed above, the value of α' is insensitive to L. Therefore, the dielectric constant ϵ of the $L=0.6$ μm crystal reaches about the same high value at T_c as the infinitely large system.[2,14,15] The dielectric constant ϵ as a function of T for various L with $t=500$ Å is shown in Fig. 8. Since the dielectric constant peaks at T_c and T_c decreases with a decreasing L, the dielectric constant at a given temperature would also peak at a certain L for which the transition temperature T_c is close to the given temperature. As an example, the dielectric constant ϵ as a function of L for $t=500$ Å at $T=15$, 25, 45, and 65 °C is plotted in Fig. 9. One can see that ϵ indeed peaks at a certain L value, similar to the experimental observations in $BaTiO_3$ ceramics.[9,10] In Fig. 10, we plot room-temperature ϵ versus L for $t=75$, 100, 167, and 500 Å. Again, the value of L at which ϵ peaks is also affected by the value for t. As t is decreased, ϵ peaks at a smaller L as similar to the change in L_c (Fig. 5).

Since most of the domain-wall studies were carried out at room temperature, the values for the domain-wall energy γ and the domain-wall thickness 2ξ in the existing literature are only suitable for room temperature. It is worth noting that both γ and ξ change substantially with temperature, especially near the bulk transition temperature $T_{c\infty}$. In Fig. 11, we plot ξ and γ versus T for a 180° domain wall that separates two semi-infinite domains. One can see that ξ tends to increase and γ tends to de-

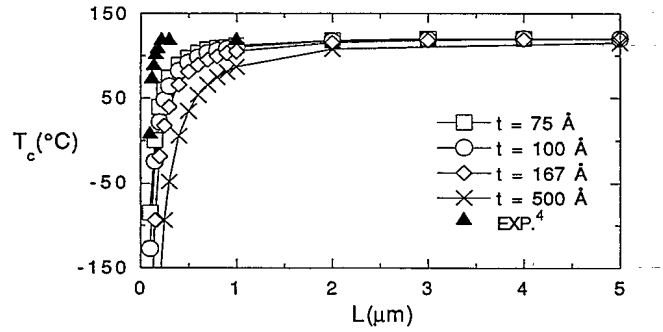

FIG. 6. T_c vs L for $t=75$, 100, 167, and 500 Å. Also plotted are the experimental values from Uchino, Sadanaga, and Hirose (Ref. 4).

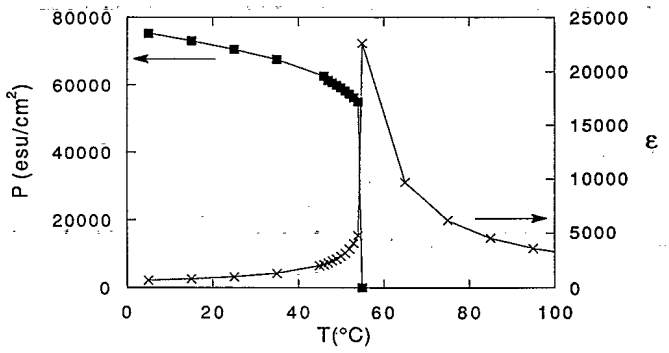

FIG. 7. P and ϵ vs T for $L=0.6$ μm and $t=500$ Å.

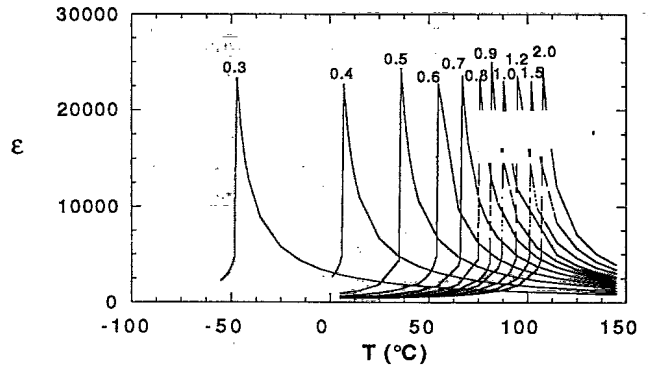

FIG. 8. ϵ vs T for various L (in μm) with $T=500$ Å.

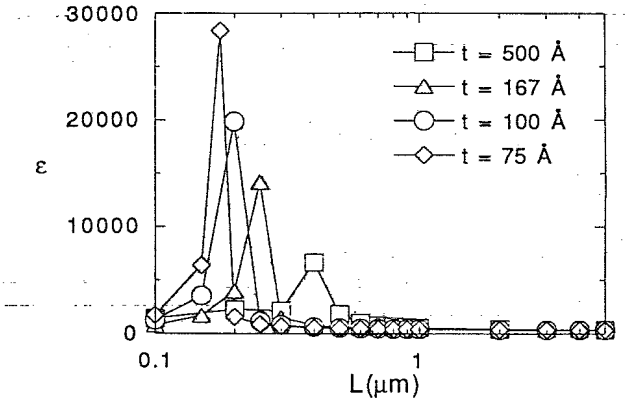

FIG. 10. ϵ vs L at $T=25$ °C for $t=75$, 100, 167, and 500 Å. Note that at a given T the peak position also changes with t.

crease with an increasing temperature, especially near $T_{c\infty}$.

The value of the polarization at the transition temperature T_c depends on the values of a', T_c-T_0, β, and σ. Both β and σ are constant, and a' and T_0 are given in Eqs. (30) and (31). A constant P at T_c, for all L, requires that $a'(T_c-T_0)$ be a constant. We found that for all L, T_c-T_0 is about 8 °C, roughly a constant. Meanwhile, even though the ratio ξ/D tends to increase with an increasing T, it generally remains small at T_c as can be seen in Fig. 12, where we plot ξ/D $(T=T_c)$ versus L for $t=75$, 100, 167, and 500 Å. Therefore, a' remains more or less constant at T_c. The constant a' at T_c together with the constant T_c-T_0 gives the constant drop of P at T_c as shown in Fig. 4.

Note that even though for larger particles ξ/D at T_c is small and tends to increase with a decreasing L, for smaller particles, i.e., $L\leq 1$ μm, ξ/D at T_c saturates at a constant value of about 0.145. It is interesting to note that the range $L\leq 1$ μm where ξ/D at T_c is constant is also the range where T_c is substantially lower than the bulk transition temperature $T_{c\infty}$. Therefore, one may think of this constant ξ/D ratio at T_c as a ferroelectric analog of the Lindemann criterion for melting, which states that at the melting temperature the ratio $\sqrt{\Delta x^2}/\bar{x}$ in a solid reaches a constant value where $\sqrt{\Delta x^2}$ is the root-mean-square displacement and $\bar{x}$ the mean nearest-neighbor distance. In other words, when the ratio ξ/D at T_c reaches a critical value, the ferroelectric phase is no longer stable.

The saturation of the ratio ξ/D at T_c in small particles sets the limit as to how small the domain width D can get and helps explain why smaller particles have a lower T_c or why at a given temperature there is a critical size L_c below which the ferroelectric phase is absent. For example, the explanation for the latter may be given as follows. At a given T, the domain width D decreases with a decreasing L as shown in Fig. 13, where D at room temperature is plotted versus L for $t=75$, 100, 167, and 500 Å. Meanwhile, at a given T, ξ does not change very much with a decreasing L as shown in Fig. 14, where ξ as a function of L for $t=75$, 100, 167, and 500 Å is plotted. As a result, at a given T, the ratio ξ/D increases with a decreasing L as shown in Fig. 15, where the room-temperature ξ/D for $t=75$, 100, 167, and 500 Å is plotted as a function of L. On the other hand, the saturation of ξ/D at around 0.145 at T_c shown in Fig. 12 indicates that there is a limit on how small D can be. The intercepts of the extrapolated curves of ξ/D with the dashed

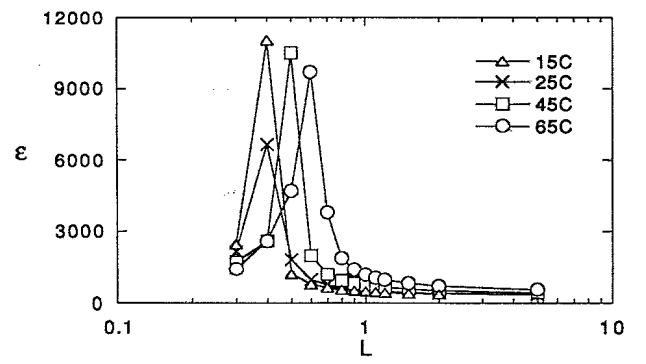

FIG. 9. ϵ vs L (in μm) at $T=15$, 25, 45, and 65 °C with $t=500$ Å. Note that ϵ peaks at a certain L whose T_c is close to the given temperature.

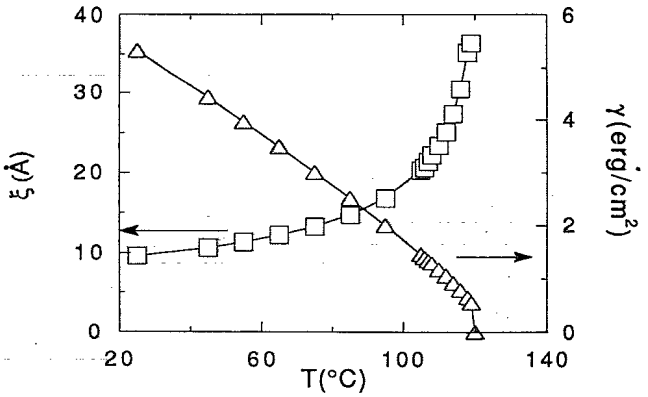

FIG. 11. Half domain-wall thickness ξ and domain-wall energy γ as a function of temperature. Note that both ξ and γ change substantially near $T_{c\infty}$, where $T_{c\infty}$ is the bulk transition temperature.

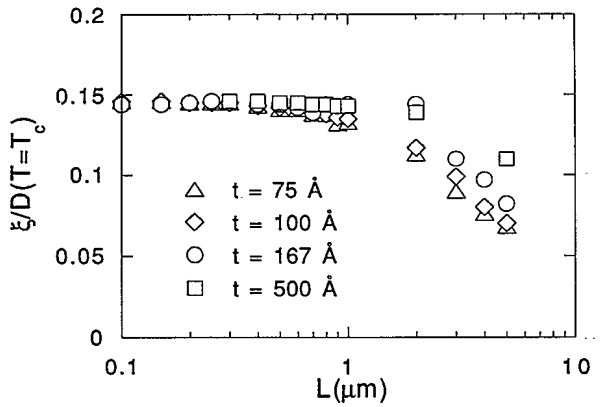

FIG. 12. ξ/D ($T=T_c$) vs L. Note that for small L, ξ/D at T_c reaches a constant value of about 0.145, which may be thought of as an analog of the Lindemann rule.

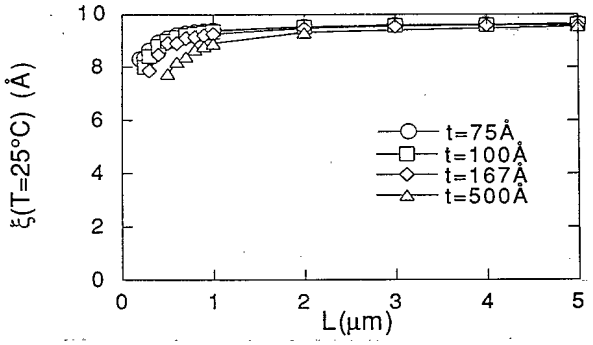

FIG. 14. ξ ($T=25$ °C) vs L for $t=500$, 167, 100, and 75 Å.

line at $\xi/D=0.145$ gives the critical sizes L_c at room temperature, which are 0.45, 0.26, 0.2, and 0.175 μm for $t=500$, 167, 100, and 75 Å. Below L_c, the extrapolated D would give a ξ/D ratio larger than 0.145. Therefore, the ferroelectric phase becomes unstable for $L \leq L_c$ at room temperature. Similarly, the ξ/D ratio of the smaller particles reaches the constant value 0.145 at a lower temperature, giving rise to the lower T_c of the smaller particles.

Finally, for the present calculations, in the bracket on the right-hand side of Eq. (31) can be neglected and Eq. (31) can be reduced as

$$T_0 = T_{0\infty} - \frac{1}{a'}\left[1.7\frac{Dt}{L^2}\right] . \tag{33}$$

Equation (33) describes how the Curie-Weiss temperature of small particles changes with the particle size L. Since a' is independent of L as we have discussed above, for a constant t, it follows from Eq. (33) that $\Delta T_0 = T_0 - T_{0\infty}$ is proportional to D/L^2. Meanwhile, since $T_c - T_0 \cong 8°$ for all L, it follows that $\Delta T_c \propto D/L^2$. In Figs. 16 and 17, we plot ΔT_c and D ($T=T_c$) as a function of L, respectively, where $\Delta T_c = T_c - T_{c\infty}$, with $T_{c\infty}$ denoting the transition temperature of an infinitely large crystal. D ($T=T_c$) as a function of L can be fitted as D ($T=T_c$) $\propto L^{0.7}$, and ΔT_c is indeed proportional to D ($T=T_c$)$/L^2$ as $L^{-1.3}$. Note that at room temperature D increases linearly with L as shown in Fig. 13 instead of D ($T=T_c$) $\propto L^{0.7}$ as shown in Fig. 17. The difference is that D ($T=T_c$) is taken at the transition temperature of each L, whereas the room-temperature D shown in Fig. 13 is taken at a fixed temperature for all L. The linear dependence of the room-temperature D with respect to L is a result of using the Schottky type of space-charge layer as discussed above.

IV. CONCLUDING REMARKS

We have examined the effect of depolarization on the ferroelectric transition of small $BaTiO_3$ particles. To reduce the depolarization energy, particles break up into domains of different polarization. The depolarization energy, which includes both the energy due to the depolarization field and the domain-wall energy, was incorporated into the Landau-Ginzburg free energy. Furthermore, to take into account that $BaTiO_3$ is not perfectly insulating, a Schottky-type space-charge layer about a few hundred Å thick as estimated by many researchers was considered. The domain-wall energy is calculated within Landau-Ginzburg theory by assuming a hyperbolic

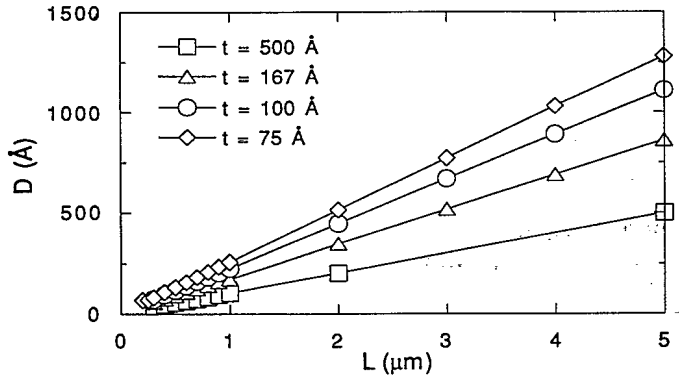

FIG. 13. D ($T=25$ °C) vs L for $t=500$, 167, 100, and 75 Å.

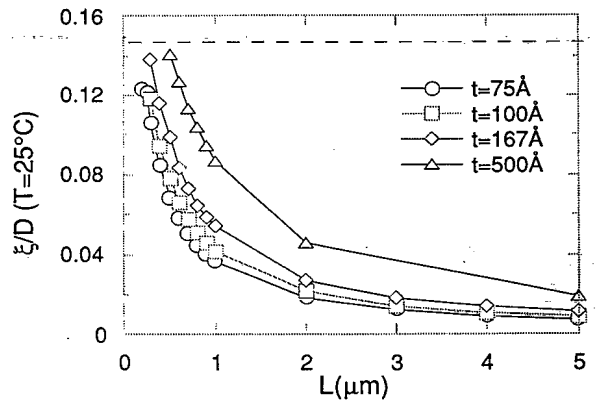

FIG. 15. ξ/D ($T=25$ °C) vs L for $t=500$, 167, 100, and 75 Å.

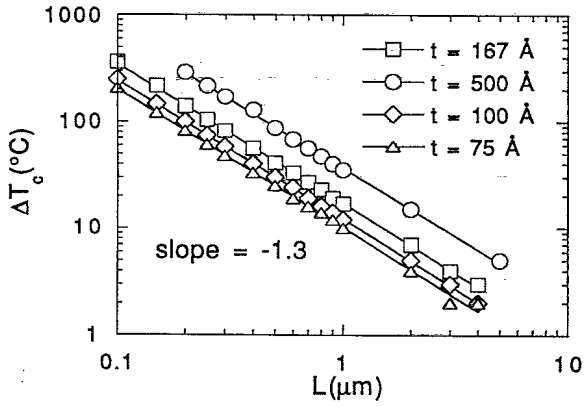

FIG. 16. ΔT_c vs L for $t=500$, 167, 100, and 75 Å.

tangent polarization profile and by minimizing the domain-wall energy with the domain-wall thickness.

We showed that with a Schottky space-charge layer 75–500 Å thick the polar phase becomes unstable for cubic particles smaller than 0.2–0.5 μm at room temperature, depending on the space-charge layer thickness, in line with many experimental observations.[4,6,7] In addition, the polarization of small particles at a constant temperature decreases with a decreasing particle size, in agreement with the experimental result that the tetragonality $(c/a-1)$ of small particles decreases with a decreasing particle size.[1,4] Meanwhile, we also showed that the polarization at T_c is constant regardless of the cubic particle size, which is in line with the experimental observation of a constant value of c/a at T_c for various particle sizes.[4] It was also shown that the domain width D decreases with the cubic particle size, which agrees with the TEM observation of the 90° domain walls in $BaTiO_3$ ceramics,[9] although 180° domain walls were considered in this study. Because of the size dependence of T_c, at a given temperature, the dielectric constant peaks at a certain cubic particle size at which the transition temperature T_c is closest to that temperature. This result agrees with the observation in $BaTiO_3$ ceramic samples.[9]

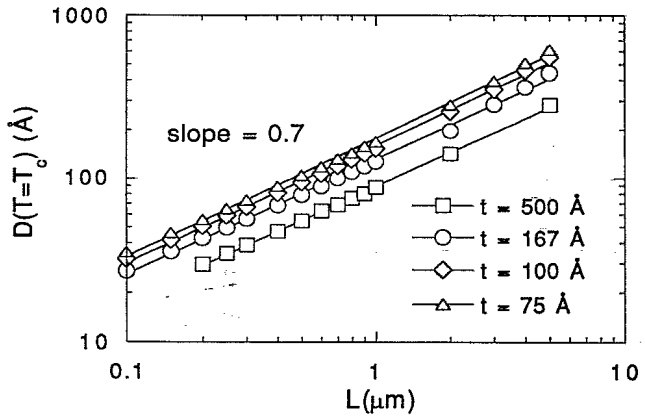

FIG. 17. $D(T=T_c)$ vs L for $t=500$, 167, 100, and 75 Å.

In principle, for a given bulk charge-carrier concentration, one can calculate the Schottky-layer thickness by solving the Poisson (or Poisson-Boltzmann) equation for the actual charge-carrier distribution in the particle,[13,22] which was not done in the present paper. However, we can estimate the charge-carrier concentration within the layer, which is related to the charge-carrier concentration within the particle. Assuming a Schottky-type layer, the carrier concentration within the layer can be estimated by $n=\rho/e$, where ρ is the charge density in the layer as depicted in Eq. (7) and e the electronic charge. With $P=78\,000$ esu/cm^2 at room temperature, $n\cong 3\times 10^{19}$ and 2×10^{20} cm^{-3} for $t=500$ and 75 Å, respectively. The space-charge layer thickness t decreases with an increasing charge-carrier concentration in the layer. The charge-carrier concentration within the layer should increase with an increasing charge-carrier concentration in the particle. Therefore, a smaller t represents a higher charge-carrier concentration (i.e., higher conductivity) in the particle.

Generally, the theory works for semiconductors down to insulators. As the conductivity of the material is parametrized by the Schottky-layer thickness t, a smaller t represents a higher bulk charge-carrier concentration in the particle. For particles with a Schottky-layer thickness $t<L$, the depolarization energy is reduced by a factor of t/L as discussed in the text. In the case of insulators, one may think that t is so large that $t>L$ for all L. Therefore, the depolarization field exists in the entire particle and there is no reduction in the depolarization energy; i.e., the t/L factor is replaced by L/L.

In addition, the present theory should be applicable to all small ferroelectric particles regardless of the mechanism of the ferroelectric transition. The reason is that the depolarization effect which is the focus of the present theory is independent of the transition mechanism. As long as there is polarization, there is a depolarization field regardless of how the polarization comes about. Meanwhile, Landau-Ginzburg theory, which is the foundation of the present theory, does not address the transition mechanism either. It only describes the ferroelectric transitions by expanding the free energy in terms of the polarization. With different values for the coefficients in the free-energy expansion, Landau-Ginzburg theory is applicable not only to perovskite ferroelectrics, but also to KDP whose transition mechanism is different from that of the perovskite ferroelectrics. Thus the present theory can be readily applied to other ferroelectric materials such as KDP or $PbTiO_3$ provided that the coefficients in the Landau-Ginzburg free energy for these materials are known.

It should be noted that some ferroelectric materials may have more than one ferroelectric phase. For example, $BaTiO_3$ can transform from the tetragonal phase to another ferroelectric phase (i.e., the orthorhombic phase) at a lower temperature. The present theory only deals with the effect of particle size on the paraelectric-to-ferroelectric transition. We did not consider the transition among different ferroelectric phases at the moment, although the effect of particle size on the transition among different ferroelectric phases is also an interesting

problem.

Experimentally, the depolarization effect on small $BaTiO_3$ particles can be examined by embedding the small $BaTiO_3$ particles in both an insulating medium and a conducting medium as has been done for small KDP particles.[14] The difference in the XRD and dielectric constant measurements on the two types of composites would be the result of the depolarization effect.

Besides the depolarization effect examined in this paper, the contribution of the stress development is also important in ceramic samples and thin films.[30] The present theory is more applicable to powders since stress development is less likely in powders than in ceramic samples or thin films. To take into account the stress effect or the presence of 90° domain walls, a Devonshire type of theory[27] will be needed.

Finally, it is worth mentioning again that the depolarization effect on the ferroelectric transition of small ferroelectric particles has no counterpart in ferromagnetic crystals, as the magnetostatic self-energy is about 10^3 times smaller than the transition energy and thus cannot suppress the spontaneous magnetization.[14]

ACKNOWLEDGMENTS

We gratefully acknowledge the financial sponsorship from the Air Force Office of Scientific Research under AFOSR Grant No. F49620-93-1-0259. Additional support by Drexel University for W.-H. Shih is also acknowledged.

[1]M. Anliker, H. R. Brugger, and W. Känzig, Helv. Phys. Acta **27**, 99 (1954).
[2]W. Känzig, *Ferroelectrics and Antiferroelectrics* (Academic, New York, 1957), p. 58.
[3]K. Ishikawa, K. Yoshikawa, and N. Okada, Phys. Rev. B **37**, 5852 (1988).
[4]K. Uchino, E. Sadanaga, and T. Hirose, J. Am. Ceram. Soc. **72**, 1555 (1989).
[5]K. Saegusa, W. E. Rhine, and H. K. Bowen, J. Am. Ceram. Soc. **76**, 1505 (1993).
[6]F. Dogan, C. M. Chun, and I. A. Aksay (unpublished).
[7]W.-H. Shih and Q. Lu, Ferroelectrics **154**, 241 (1994).
[8]M.-H. Lee, A. Halliyal, and R. E. Newnham, Ferroelectrics **87**, 71 (1988).
[9]G. Arlt, D. Hennings, and G. de With, J. Appl. Phys. **58**, 1619 (1985).
[10]See the references cited in Ref. 9.
[11]For example, see J. Paletto, G. Grange, R. Goutte, and L. Eyraud, J. Phys. D **7**, 78 (1974).
[12]G. A. Samara, Phys. Rev. **151**, 378 (1966).
[13]I. P. Batra, P. Wurfel, and B. D. Silverman, Phys. Rev. B **8**, 3257 (1973).
[14]F. Jona and G. Shirane, *Ferroelectric Crystals* (Dover, New York, 1962).
[15]E. Fatuzzo and W. Merz, *Ferroelectricity* (North-Holland, Amsterdam, 1967).
[16]W. Merz, *Progress in Dielectrics* (Academic, New York, 1962), Vol. 4.
[17]F. S. Galasso, *Structure, Properties and Preparation of Perovskite Compounds* (Pergamon, New York, 1969).
[18]S. Chikazumi, *Physics of Magnetism* (Wiley, New York, 1964), p. 554.
[19]W. Känzig, Phys. Rev. **98**, 549 (1955).
[20]For example, see *Metal-Semiconductor Schottky Barrier Junctions and Their Applications,* edited by B. L. Sharma (Plenum, New York, 1984).
[21]S. Triebwasser, Phys. Rev. **118**, 100 (1960).
[22]P. E. Bloomfield, I. Lefkowitz, and A. D. Aronoff, Phys. Rev. B **4**, 974 (1971).
[23]W. J. Merz, Phys. Rev. **95**, 690 (1954).
[24]W. Kinase and H. Takahashi, J. Phys. Soc. Jpn. **12**, 464 (1957).
[25]W. Kinase, Prog. Theor. Phys. (Kyoto) **13**, 529 (1955).
[26]V. A. Zhirnov, Z. Eksp. Theor. Fiz. **35**, 1175 (1959) [Sov. Phys. JETP **8**, 822 (1959)].
[27]A. F. Devonshire, Philos. Mag. **42**, 1065 (1951); **40**, 1040 (1949).
[28]W. Cao and E. Cross, Phys. Rev. B **44**, 5 (1991).
[29]X. Zhang and D. C. Joy, Appl. Phys. Lett. **60**, 787 (1992).
[30]B. S. Kwak, A. Erbil, B. J. Wilkens, J. D. Budai, M. F. Chisholm, and L. A. Boatner, Phys. Rev. Lett. **68**, 3733 (1992).